# Evaluation of the coracoid bone tunnel placement on Dog Bone button fixation for acromioclavicular joint dislocation: a cadaver study combined with finite element analysis

**Rangshan Gao**
Dalian Medical University
**Wendong Zhang**
Northern Jiangsu People's Hospital, Yangzhou University
**Yuxia Yang**
Dalian Medical University
**Yucheng Zhang**
Dalian Medical University
**Yangyang Hu**
Northern Jiangsu People's Hospital, Yangzhou University
**Honghai Wu**
Northern Jiangsu People's Hospital, Yangzhou University
**Mingsheng Liu**
Northern Jiangsu People's Hospital, Yangzhou University
**Wenyong Fei**
Northern Jiangsu People's Hospital, Yangzhou University
**Jingcheng Wang** ( sbydyxwjc@163.com )
Northern Jiangsu People's Hospital, Yangzhou University

**Research Article**

**Keywords:** Acromioclavicular joint dislocation, Dog Bone, Finite element analysis, Tunnel location, Cadaver study

**Posted Date:** June 22nd, 2022

**DOI:** https://doi.org/10.21203/rs.3.rs-1756852/v1

# Abstract

**Background:** Dog Bone button fixation was frequently used to treat acromioclavicular joint (ACJ) dislocation. However, there were many studies reporting about complications after fixation.

**Objective:** To investigate the effect the coracoid bone tunnel location had on the treatment of ACJ dislocation using a single-tunnel coracoclavicular (CC) ligaments fixation with the Dog Bone button.

**Methods:** Six cadaveric shoulders were used. Each specimen underwent five testing conditions, performed in the following order: (1) normal ACJ (Gn). (2) The acromioclavicular and CC ligaments were removed (G0). (3) The CC ligament reconstruction was performed using the Dog Bone technique and the coracoid bone tunnel was at the center of the coracoid base (G1), or (4) 5 mm distal from the G1 site, along the axis of the coracoid (G2), or (5) 10 mm distal from the G1 site, along the axis of the coracoid (G3). The angles of pronation and supination of the clavicles under the same load (30 N) were measured. Next, a finite element (FE) model was created by using computed tomography (CT) images from the normal shoulder. Model 1 (M1), model 2 (M2), and model 3 (M3) correspond to G1, G2, and G3, respectively. A force of 70 N was used as a vertical upward load added to the distal clavicle. Consequently, the von Mises stress and the strain LE along the FiberWire and the displacement nephogram of the three models have been obtained.

**Results:** After single-tunnel CC ligaments fixation using the Dog Bone technique, the clavicles in group G2 (20.50 (19.50, 21.25) °, 20.00 (18.75, 21.25) °) were the most stable ($P < 0.001$). The peak von Mises stress and the strain LE along the FiberWire, and the maximum displacement in M2 were all smaller than in M1 and M3.

**Conclusions:** When the coracoid bone tunnel is located 5 mm anterior to the center of the coracoid base (along the axis of the coracoid), the clavicle gained greater stability.


# Background

An ACJ dislocation is a common shoulder injury, which accounts for approximately 12% of all shoulder dislocations. The treatment options depend upon the degree of the ACJ dislocation. Indeed, a Rockwood type □-□ dislocation is usually treated with surgery. However, surgical intervention for a Rockwood type □ dislocation remains a widely discussed topic of debate. Previous literature suggests that surgical treatment can be considered for patients who undertake a high demand for activity, such as young competitive athletes[1–4]. A wide variety of surgical techniques has been described for the surgical treatment of ACJ dislocations, with many focusing on the reconstruction of the injured CC ligaments[5].

The single-tunnel CC ligaments fixation of a dislocated ACJ using the Dog Bone represents a current clinical method of treatment. This technique aims to restore the level of strength and stability similar to the original anatomy, which will allow the patients to achieve painless shoulder movement without any restriction of movement[6]. However, previous clinical studies have reported complication rates from CC

ligament reconstruction techniques ranging from 23–80%[5, 7–9]. The CC ligament reconstruction using a coracoid bone tunnel technique presents visualization challenges and a high degree of difficulty, leading to reports detailing that those surgeons performing this technique undergo ‘a steep learning curve’. Therefore, it is not surprising that iatrogenic complications, such as coracoid and clavicle fractures, occur from drilling in the coracoid[5]. However, relatively few studies exist that have attempted to identify the ideal tunnel location in the coracoid for the Dog Bone button fixation. One biomechanical study using synthetic bone models demonstrated that the risk of a coracoid fracture decreases following the placement of holes at the coracoid base[10]. Further work using computer simulations has shown that drilling at the base of the coracoid may reduce the risk of an intraoperative coracoid fracture[11]. However, they failed to consider the factors of the clavicles and did not conduct any further studies on the mechanisms underlying the effects of the different coracoid bone tunnels positions on coracoid and clavicle fractures.

To our knowledge, there is currently limited evaluation of the effect of the coracoid bone tunnel location on the clavicle following a single-tunnel reconstruction of the CC ligament using Dog Bone buttons. Therefore, this experiment was established to investigate the relationship between them. Our hypothesis was that the clavicle gained increased stability when the coracoid bone tunnel is located 5 mm anterior to the center of the coracoid base (along the axis of the coracoid). Concurrently, this study also aimed to contribute to the understanding of the mechanisms by which the different locations of the coracoid bone tunnels affected the coracoid and clavicle fractures.

To achieve these aims, this study implemented cadaver studies and finite element analysis (FEA), which is a branch of biomechanical research commonly used in engineering and dentistry. Moreover, FEA is currently widely used in medical research owing to its biomechanical properties as a non-invasive, low-cost, and high validity method.

## Materials And Methods

## Cadaveric study

## Specimen preparation

Six cadaver shoulders were used (two males and one female, all of whom died of non-orthopedic causes; mean age of 53.3 years; ranging from 45 to 62 years). All soft tissues of the ACJ in the cadavers were stripped and the ACJ anatomy was observed. The specimens were kept moist throughout the experiment via a 0.9% normal saline[5].

## Coracoid and Clavicle Tunnel Location for the Dog Bone Fixation

The clavicle bone tunnel is located in the middle, approximately 35 mm from the distal end of the clavicle (Fig. 1A)[8, 12]. The middle of the coracoid base was identified by measuring the medial-lateral length of

the base's superior aspect with digital calipers. The midpoint was determined and used as the landmark for tunnel placement. The three drilling locations of the coracoid bone tunnel are: firstly, one is located centrally at the base of the coracoid (G1). The second is 5 mm distal along the long axis of the coracoid from the G1 site (G2), while the third is 10 mm distal along the long axis of the coracoid from the G1 site (G3) (Fig. 1B & C)[4, 5].

# Single-tunnel fixation of the ACJ dislocation using the Dog Bone technique

The Burkhart-Dog Bone button single bundle reconstruction technique was implemented for the surgical reparation of the ACJ dislocations. This technique used two buttons and a FibeWire (Arthrex, USA) to reconstruct the CC ligament (Fig. 2A, B & C).

# Methods and Indicators of the Cadaveric study

The cadaveric study was performed on each shoulder under five conditions. A normal ACJ (Gn), then in G0-G3, where the acromioclavicular and CC ligaments had been cut off to simulate a type □-□ ACJ dislocation. Moreover, no buttons were used for the CC ligaments reconstruction (G0). In G1-G3, the CC ligament reconstruction was performed using the Dog Bone technique, whereby the clavicle bone tunnel was located in the middle site, approximately 35 mm from the distal end of the clavicle. However, the coracoid bone tunnel was either at the center of the coracoid base (G1), 5 mm distal from the G1 site, along the axis of the coracoid (G2), or 10 mm distal from the G1 site and along the axis of the coracoid (G3).

Firstly, a kirschner wire with a 3 mm diameter was fixed in the middle of the clavicle. The kirschner wire was then placed in a sleeve and a force-measuring device was used 10 cm from the top of the sleeve to apply a 30 N pulling force perpendicular to the sleeve and in the direction of the cadaver's foot and head, respectively. The clavicle subsequently produced pronation and supination movements under the force. Finally, the angle of the kirschner wire was measured using a goniometer, while the distance between the two buttons was measured under different conditions (Fig. 3A, B, C & D).

# FE analysis

# Three-dimensional geometry of the scapula and clavicle

A healthy male volunteer (49 years old) was selected, and the clavicle fracture, scapula fracture, scapula, and clavicle deformity were excluded. Informed consent was signed, and the patient underwent a CT scan of the shoulder joint. Scanning parameters: scanning voltage 140 kV, scanning current 145 mA, matrix 512x512px, layer thickness and layer spacing 1.25 mm, 345 thin-layer images were obtained. The thin-layer images were saved in DICM format and output by the PACS system, then imported into Mimics19.0 software. After threshold adjustment, image mask segmentation, and other operations, 2D masks of the

scapula and clavicle were obtained. Then 3D reconstruction of 2D masks was carried out to obtain 3D models of scapula and clavicle, which were exported as STL format files. Reverse surface operation: import the STL model of scapular and clavicle into GeomagicsStudio2012 software, smooth the model by filling the void and removing the features. Enter the precise surface module, after detecting the contour, and constructing the curved surface and grid, the model is transformed into a solid geometry file, which is saved and exported in STEP format (to simplify calculations, all soft tissues were excluded) (Fig. 4A, B & C)[11, 13].

# Three-dimensional models of the Dog Bone button and the FiberWire

Assemble the Dog Bone internal fixation models to the bone models: according to the parameters of the Dog Bone internal fixation models provided by the manufacturer, draw the three-dimensional models of button internal fixation in SolidWorks software, and the FiberWire was replaced by a cylinder with a diameter of 3 mm, and simplify the models appropriately (Fig. 4D)[3].

# Three-dimensional model of Dog Bone button for ACJ dislocation

We have imported the geometric models of the above four kinds of assembly (button; FibeWire; scapula and clavicle) into hypermesh14.0 software, and then carried out mesh division and material attribute assignment. All parts were C3D4 units and imported into abaqus6.14 software in INP format. Based on cadaver studies, we introduced Dog Bone internal fixation models into bone models to simulate CC ligament reconstruction under the G1, G2, and G3 (Fig. 4E).

# Material properties, Load condition, and Boundary conditions

The material properties incorporated into this study were two independent parameters: Young's modulus (E) and Poisson's ratio (v) (Table 1). All bones and implants were assumed to be homogeneous, isotropic, and linearly elastic. Biomechanical properties of bones, implants, buttons, and the FiberWire were applied to the models[6, 14, 15].

Table 1
Material properties of the models

| Material | Young's modulus (MPa) | Poisson's ratio |
|---|---|---|
| Bone | 17000 | 0.30 |
| Button | 96000 | 0.36 |
| FiberWire | 3800 | 0.28 |
| NOTE. MPa, MegaPascals. | | |

The load and boundary conditions used in the present study were derived from those used in a previous study. The sternal articular surface of the clavicle and the inferior surface of the acromion were determined for the boundary conditions (Fig. 5)[3, 13, 16, 17]. FiberWire was bonded with buttons (TIE). Friction contact was taken between the FiberWire and the clavicular bone tunnel and coracoid bone tunnel, and the contact factor was 0.46. Two buttons were subjected to frictional contact with bone with a contact factor of 0.36. Constrained all degrees of freedom of the subacromial node to fix the scapula. The joints of the proximal clavicle were coupled to the center of the articular surface, constrained U1, U2, and U3 degrees of freedom of the center, and retained UR1, UR2, and UR3 degrees of freedom to achieve limited sliding of the proximal clavicle in the sternoclavicular joint. The load condition was the external upward force (70 N) that acted on the distal clavicular area and simulated the stresses of mild physical rehabilitation[18–20]. Finally, we obtained the displacement nephogram of the three models and the peak value of von Mises stress and the strain LE along the FiberWire.

# Statistical analysis

Statistical analysis was performed by SPSS 26.0 (SPSS Inc., Chicago, IL) software. SW test was performed to determine whether the data was in accordance with the normal distribution. The data in accordance with the normal distribution was expressed as the mean ± standard deviation and data did not conform to the normal distribution was expressed as the median (25% quartile, 75% quartile). Kruskal-Wallis test was used to determine the difference among groups. The difference among groups was considered significant when $P < 0.05$.

## Results

# The cadaveric study

The results of the cadaveric study were summarized (Table 2). Pairwise comparison between Gn, G0, G1, G2 and G3 (Table 3). From Table 3, we can see that there was no significant difference between the G2 and Gn groups, while there was a significant difference between the G2 and G0 groups.

Table 2
Results of the cadaveric study

| | Gn | G0 | G1 | G2 | G3 | P value |
|---|---|---|---|---|---|---|
| Angles of pronation (°) | 14.50 (12.75, 15.25) | 48.00 (43.50, 52.00) | 27.50 (25.50, 28.50) | 20.50 (19.50, 21.25) | 35.00 (32.75, 37.00) | P < 0.001 |
| Angles of supination (°) | 14.50 (13.00, 15.25) | 47.50 (42.75, 52.00) | 28.00 (26.50, 30.00) | 20.00 (18.75, 21.25) | 36.00 (34.75, 36.50) | P < 0.001 |
| The distances between the two buttons (mm) | None | None | 38.00 (37.00, 39.25) | 34.50 (33.75, 35.25) | 38.50 (37.75, 39.25) | P = 0.003 |
| NOTE. Data presented as the median (25% quartile, 75% quartile). | | | | | | |

°, Degree sign.

mm, Millimeter.

None, no buttons were used for the CC ligaments reconstruction.

Table 3
Pairwise comparison of pronation and supination angles between Gn, G0, G1, G2 and G3

| | Gn-G2 | Gn-G1 | Gn-G3 | Gn-G0 | G1-G2 | G2-G3 | G0-G2 | G1-G3 | G0-G1 | G0-G3 |
|---|---|---|---|---|---|---|---|---|---|---|
| Pronation angles | P = 1.000 | P = 0.181 | P = 0.004 | P < 0.001 | P = 1.000 | P = 0.181 | P = 0.004 | P = 1.000 | P = 0.181 | P = 1.000 |
| Supination angles | P = 1.000 | P = 0.181 | P = 0.004 | P < 0.001 | P = 1.000 | P = 0.181 | P = 0.004 | P = 1.000 | P = 0.181 | P = 1.000 |
| NOTE. *Significant difference between the G2 and G0 groups (P = 0.004). | | | | | | | | | | |

# The FEA

**The displacement nephogram.** Following the application of a loaded force to the distal end of the clavicle, the displacement nephogram of the FE models illustrated a maximum displacement of M1 located at the front of the clavicle's distal end (1.5610 mm). The maximum displacement of M2 was located at the middle position of the distal end (0.4244 mm), while the maximum displacement of M3 was located behind the distal end (2.4420 mm) (Fig. 6).

**The peak von Mises stress.** The peak value of the von Mises stress along the FiberWire in M1 was 121.70 MPa, while in M2 it was 33.11 MPa, and M3 produced 64.71 MPa (Fig. 7).

**Strain LE.** The strain LE along the FiberWire in M1 was 0.010080, while in M2 it was 0.006227, and finally, in M3 it was 0.017090 (Fig. 8).

The loading values were summarized in Table 4.

Table 4
A summary of the FEA results

| | Maximum displacements (mm) | The peak values of von Mises stress (MPa) | Strain LE |
|---|---|---|---|
| M1 | 1.5610 | 121.70 | 0.010080 |
| M2 | 0.4244 | 33.11 | 0.006227 |
| M3 | 2.4420 | 64.71 | 0.017090 |
| NOTE. mm, Millimeter. | | | |

MPa, MegaPascals.

# Discussion

This study aimed to investigate the effect the coracoid bone tunnel location had on the treatment of ACJ dislocation using a single-tunnel CC ligaments fixation with the Dog Bone button. Firstly, a cadaveric study was performed, followed by the implementation of FEA to further prove the validity of the cadaver study results. Overall, when the coracoid bone tunnel is located 5 mm anterior to the center of the coracoid base (along the axis of the coracoid), the clavicle gained greater stability.

Previously, several postoperative complications have been reported following a single-tunnel CC ligament reconstruction of an ACJ dislocation using the Dog Bone technique. Shin et al.[21] reported a 33% rate of loss of reduction of more than 50% in 18 patients managed with a single-tunnel, adjustable-loop suspensory device. Cook et al.[22] reported that in 8 of 10 repairs (80%) intraoperative reduction was lost at an average of 7.0 weeks (range, 3–12 weeks), and four patients (40%) required revisions. Tunnel widening was universally noted, and the holding suture was prominently described as the failure mode in most patients. Dalos et al.[23] reported that tunnel widening was observed for Dog Bone technique and was located in the inferior parts of the clavicle and superior parts of the coracoid. However, the specific reason of postoperative tunnel widening remain unclear. Therefore, our findings provide novel information regarding a potential explanation.

Firstly, the cadaver study data detail that for G2, the angles of pronation and supination of the clavicle were 20.50 (19.50, 21.25) °, 20.00 (18.75, 21.25) °, respectively. There was no significant difference between the G2 and Gn groups, while there was a significant difference between the G2 and G0 groups. This means that the clavicle of group G2 appeared more stable in response to an external force. Additionally, the distances between the two buttons in group G2 (34.50 (33.75, 35.25) mm) were also

smaller than in groups G1 (38.00 (37.00, 39.25) mm) and G3 (38.50 (37.75, 39.25) mm), which further explains why the group G2 clavicle appeared more stable in response to an external force.

Subsequently, FEA was implemented and the displacement nephogram of FE models shows that the maximum displacement of M1 was located in front of the distal end of the clavicle (1.5610 mm) and the clavicle tended to supinate. The location of M2 at the middle position of the distal end of the clavicle (0.4244 mm) and the displacement direction of the distal clavicle are almost vertical. Finally, M3 was located behind the distal end of the clavicle (2.4420 mm) and the clavicle tended to pronate. Since the coracoid bone tunnel is located in the center of the coracoid process base, it is relatively backward in M1. Thus, when the resultant force of the load was added to the distal clavicle it occurred in front of the distal clavicle, indicating that the displacement is greatest in front of the distal clavicle, which tends to supinate. For M2, the resultant force appears in the middle of the distal clavicle, so the displacement of the middle of the distal clavicle is the largest, making the distal clavicle move vertically. For M3, because the coracoid bone tunnel is located at the distal end of the coracoid process, its position is relatively forward. Therefore, the resultant force occurs behind the distal end of the clavicle, so the displacement behind the distal end of the clavicle is the largest and causes the tendency of the clavicle to pronate.

Generally, when the coracoid bone tunnel is located in the center of the base of the coracoid process or 10 mm anterior to the center of the base (along the axis of the coracoid), the action of external force promotes supination or pronation in the clavicle. This is consistent with the results of our cadaver study where the M2 clavicle appeared more stable in response to an external force. Moreover, a supination or pronation movement in the clavicle causes the FiberWire to cut the clavicular and coracoid bone tunnel, resulting in the widening of the bone tunnel. In addition, the peak value of von Mises stress and the strain LE along the FiberWire in M2 were both smaller than in M1 and M3. This indicates that M2 is the least likely to fail under the same load conditions. Hence, when the coracoid bone tunnel is located in the G1 site or 10 mm anterior to the G1 site (along the axis of the coracoid), the risk of a postoperative clavicular and coracoid fracture will be increased. Likewise, the erosion of clavicular and coracoid bone can be promoted by buttons and also increase the risk of a clavicular or coracoid button failure. These complications may directly or indirectly lead to an ACJ dislocation reduction failure or re-dislocation.

Previous investigations have analyzed the location selection of the coracoid bone tunnel. Kummer et al. [10] used a combination of synthetic bone models and cadaveric scapulae to assess the effect of tunnels on the coracoid strength. Kummer and co-authors reported that the cadaveric specimens were more prone to fracture when tunnels were placed in the distal coracoid compared to the base. Campbell et al.[5] used six matched pairs of cadaveric scapulae to study the effect of the coracoid bone tunnel position on the treatment of an ACJ dislocation using Dog Bone. They reported that the ultimate load for the centered tunnels in the distal coracoid absorbed a significantly higher ultimate load and energy compared to the eccentric tunnels. Although, they did not find a difference between the distal tunnels and the tunnels at the base. However, their study ignored the factors of the clavicles and also did not conduct further studies into the underlying mechanisms for the effects of the different coracoid bone tunnels positions on the coracoid and clavicle fractures. Our results provide a possible explanation for these underlying

mechanisms: whereby during a single-tunnel reconstruction of the CC ligament, the different positions of the coracoid bone tunnel will lead to altering stabilities of the clavicle. These will ultimately result in numerous cutting degrees of the FiberWire to the clavicle and coracoid bone tunnels. Indeed, these cuts may lead to either the clavicle and coracoid bone tunnels widening, which can promote clavicular or coracoid fractures and other postoperative related complications. Therefore, to reduce the occurrence of these complications, our suggestion is that during a single-tunnel CC ligaments fixation of an ACJ dislocation using a Dog Bone, the coracoid bone tunnel should be positioned 5 mm anterior to the center of the coracoid process base, along the axis of the coracoid.

As the research into ACJ dislocations increases, our current research aims are to explore a method that can both achieve ideal reduction and fixation alongside maximizing the recovery of ACJ mobility. Our results provide more information for orthopedic surgeons using a single-tunnel reconstruction of CC ligament with Dog Bone.

# Deficiencies of the study

Several limitations within this study should be considered. Firstly, the use of cadaveric specimens during biomechanical testing does not accurately mimic the real situation in vivo with the various forces involved. Therefore, some degree of error is likely to occur[19]. Secondly, using cadaveric specimens for biomechanical testing does not provide information relating to biological healing. Consequently, result validation could not be performed on the long-term effects of the grafts on the clavicle and coracoid processes under different experimental conditions[24]. Finally, the application of the FEA in orthopedics was limited by the simplification of the model, whereby some of the more complex anatomies in the bone modeling phase was omitted. Therefore, the results obtained are often questioned[25]. The addition of the load to the models was only performed in a single direction, which was chosen because it accurately represented the clinical situation. However, in patients the loads applied to the construction would likely be multidirectional. It is possible that loads applied in other directions could lead to earlier or other causes of reduced ACJ dislocation failure and our conclusions cannot be directly applied to these situations[5].

# Future study

Our further studies will focus on clinical application of ACJ treatment using Dog Bone buttons. Their clinical effects will be investigated.

## Conclusions

When the coracoid bone tunnel is located 5 mm anterior to the center of the coracoid base (along the axis of the coracoid), the clavicle gained greater stability.

## Abbreviations

ACJ

acromioclavicular joint
CC
coracoclavicular
FE
finite element
FEA
finite element analysis
CT
computed tomography.

# Declarations


### Acknowledgements

We would like to express our gratitude to Weishi Hong and Erkai Pang for providing support and assistance during the study.


### Author contributions

RG, WZ and JW developed the study design, performed the experiment and data analysis and wrote the manuscript. YY, YZ, YH and HW performed the experiment, data collection and data interpretation. ML and WF analyzed and interpreted the data. All authors read and approved the final manuscript.


### Funding

This research was supported by the fund from the Clinical application oriented medical innovation through the National orthopedics and sports rehabilitation clinical medical research center (contract number: 2021-NCRC-CXJJ-PY-07), the Scientific research project of Jiangsu Provincial Health and Health Commission (Item number: M2021042), and the Yangzhou social development project (Item number: YZ2021084).


### Availability of data and materials

The datasets used and/or analysed during the current study are available from the corresponding author on reasonable request.

### Ethics approval and consent to participate

This study was carried out in accordance with the Code of Ethics of the World Medical Association (Declaration of Helsinki) and approved by the Ethics Committee of Northern Jiangsu People's Hospital (Number: 2021ky308). A CT scan of the scapula and clavicle was obtained with the informed consent of the volunteer, and the relevant data were authorized for academic exchange.

### Consent for publication

Not applicable.

### Competing interests

The authors declare that they have no competing interests.

### Author details

[1]Dalian Medical University, Dalian 116044, People's Republic of China; [2]Sports Medicine Department, Northern Jiangsu People's Hospital, Clinical Medical College, Yangzhou University, Yangzhou 225001, People's Republic of China.

## References

1. *Elizabeth E Hibberd, Zachary Y Kerr, Karen G Roos, Aristarque Djoko, Thomas P Dompier, Epidemiology of Acromioclavicular Joint Sprains in 25 National Collegiate Athletic Association Sports: 2009–2010 to 2014–2015 Academic Years. Am J Sports Med, 2016. 44(10): p. 2667–2674.*
2. *Mark Pallis, Kenneth L Cameron, Steven J Svoboda, Brett D Owens, Epidemiology of acromioclavicular joint injury in young athletes. Am J Sports Med, 2012. 40(9): p. 2072–2077.*
3. *Sermsak Sumanont, Supachoke Nopamassiri, Artit Boonrod, Punyawat Apiwatanakul, Arunnit Boonrod, Chanakarn Phornphutkul, Acromioclavicular joint dislocation: a Dog Bone button fixation alone versus Dog Bone button fixation augmented with acromioclavicular repair-a finite element analysis study. Eur J Orthop Surg Traumatol, 2018. 28(6): p. 1095–1101.*
4. *L Barberis, M Faggiani, M J Calò, S Marenco, G Vasario, F Castoldi, Coracoid tunnels in open and arthroscopic treatment of acromioclavicular dislocation: an experimental cadaveric study. Musculoskelet Surg, 2022. 106(1): p. 15–19.*
5. *Sean T Campbell, Nathanael D Heckmann, Sang-Jin Shin, et al., Biomechanical evaluation of coracoid tunnel size and location for coracoclavicular ligament reconstruction. Arthroscopy, 2015. 31(5): p. 825–830.*
6. *Gabriela Lima Menegaz, Leandro Cardoso Gomide, Cleudmar Amaral Araújo, Biomechanical evaluation of acromioclavicular joint reconstructions using a 3-dimensional model based on the finite element method. Clin Biomech (Bristol, Avon), 2019. 70: p. 170–176.*
7. *Frank Martetschläger, Marilee P Horan, Ryan J Warth, Peter J Millett, Complications after anatomic fixation and reconstruction of the coracoclavicular ligaments. Am J Sports Med, 2013. 41(12): p. 2896–2903.*
8. *Matthew D Milewski, Marc Tompkins, Juan M Giugale, Eric W Carson, Mark D Miller, David R Diduch, Complications related to anatomic reconstruction of the coracoclavicular ligaments. Am J Sports Med, 2012. 40(7): p. 1628–1634.*
9. *Benedikt Schliemann, Steffen B Roßlenbroich, Kristian N Schneider, et al., Why does minimally invasive coracoclavicular ligament reconstruction using a flip button repair technique fail? An*

*analysis of risk factors and complications. Knee Surg Sports Traumatol Arthrosc, 2015. 23(5): p. 1419–1425.*

10. *Frederick J. Kummer, David C. Thut, Brian Pahk, David J. Hergan, Laith M. Jazrawi & Robert J. Meislin, Drill Holes for Coracoclavicular Ligament Reconstruction Increase Coracoid Fracture Risk. Shoulder & Elbow, 2017. 3(3): p. 163–165.*
11. *Robert M Coale, Scott J Hollister, Joshua S Dines, Answorth A Allen, Asheesh Bedi, Anatomic considerations of transclavicular-transcoracoid drilling for coracoclavicular ligament reconstruction. J Shoulder Elbow Surg, 2013. 22(1): p. 137–144.*
12. *Joong-Bae Seo, Dong-Ho Lee, Kyu-Beom Kim, Jae-Sung Yoo, Coracoid clavicular tunnel angle is related with loss of reduction in a single-tunnel coracoclavicular fixation using a dog bone button in acute acromioclavicular joint dislocation. Knee Surg Sports Traumatol Arthrosc, 2019. 27(12): p. 3835–3843.*
13. *Emre Çalışal, Levent Uğur, Comparison of two methods for coracoclavicular ligament reconstruction: A finite element analysis. Acta Orthop Traumatol Turc, 2020. 54(2): p. 202–206.*
14. *Cheng-Min Shih, Kui-Chou Huang, Chien-Chou Pan, Cheng-Hung Lee, Kuo-Chih Su, Biomechanical analysis of acromioclavicular joint dislocation treated with clavicle hook plates in different lengths. Int Orthop, 2015. 39(11): p. 2239–2244.*
15. *Jian-Jun Li, Dong-Mu Tian, Li Yang, Jing-Yu Zhang, Yong-Cheng Hu, Influence of a metaphyseal sleeve on the stress-strain state of a bone-tumor implant system in the distal femur: an experimental and finite element analysis. J Orthop Surg Res, 2020. 15(1): p. 589.*
16. *Onur Kocadal, Korcan Yüksel, Melih Güven, Evaluation of the clavicular tunnel placement on coracoclavicular ligament reconstruction for acromioclavicular dislocations: a finite element analysis. Int Orthop, 2018. 42(8): p. 1891–1896.*
17. *Li-Kun Hung, Kuo-Chih Su, Wen-Hsien Lu, Cheng-Hung Lee, Biomechanical analysis of clavicle hook plate implantation with different hook angles in the acromioclavicular joint. Int Orthop, 2017. 41(8): p. 1663–1669.*
18. *Lei Zhang, Ai-Ni He, Yu-Feng Jin, et al., Novel Double Endobutton Technique Combined with Three-Dimensional Printing: A Biomechanical Study of Reconstruction in Acromioclavicular Joint Dislocation. Orthop Surg, 2020. 12(5): p. 1511–1519.*
19. *Michael B Banffy, Carlos Uquillas, Julie A Neumann, Neal S ElAttrache, Biomechanical Evaluation of a Single- Versus Double-Tunnel Coracoclavicular Ligament Reconstruction With Acromioclavicular Stabilization for Acromioclavicular Joint Injuries. Am J Sports Med, 2018. 46(5): p. 1070–1076.*
20. *Steven Struhl, Theodore S Wolfson, Frederick Kummer, Axial-Plane Biomechanical Evaluation of 2 Suspensory Cortical Button Fixation Constructs for Acromioclavicular Joint Reconstruction. Orthop J Sports Med, 2016. 4(12): p. 2325967116674668.*
21. *Sang-Jin Shin, Nam-Ki Kim, Complications after arthroscopic coracoclavicular reconstruction using a single adjustable-loop-length suspensory fixation device in acute acromioclavicular joint dislocation. Arthroscopy, 2015. 31(5): p. 816–824.*

22. *Jay B Cook, James S Shaha, Douglas J Rowles, Craig R Bottoni, Steven H Shaha, John M Tokish, Early failures with single clavicular transosseous coracoclavicular ligament reconstruction. J Shoulder Elbow Surg, 2012. 21(12): p. 1746–1752.*
23. *D Dalos, G Huber, Y Wichern, et al., Acromioclavicular joint suture button repair leads to coracoclavicular tunnel widening. Knee Surg Sports Traumatol Arthrosc, 2022.*
24. *Daichi Morikawa, Augustus D Mazzocca, Elifho Obopilwe, et al., Reconstruction of the Acromioclavicular Ligament Complex Using Dermal Allograft: A Biomechanical Analysis. Arthroscopy, 2020. 36(1): p. 108–115.*
25. *Magdalena Lisiak-Myszke, Dawid Marciniak, Marek Bieliński, Hanna Sobczak, Łukasz Garbacewicz, Barbara Drogoszewska, Application of Finite Element Analysis in Oral and Maxillofacial Surgery-A Literature Review. Materials (Basel), 2020. 13(14).*

# Figures

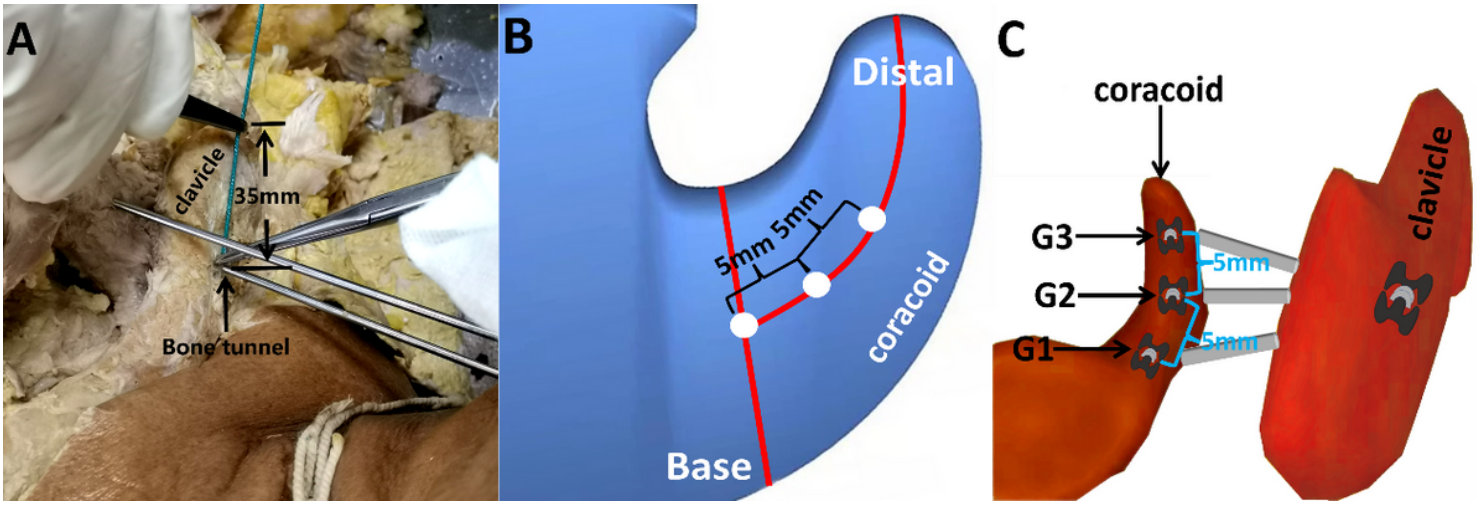


**Figure 1**

The location of the clavicle bone tunnel (A). Pattern diagram of the coracoid bone tunnel location. The white dots represent the locations of the coracoid bone tunnels (B & C).

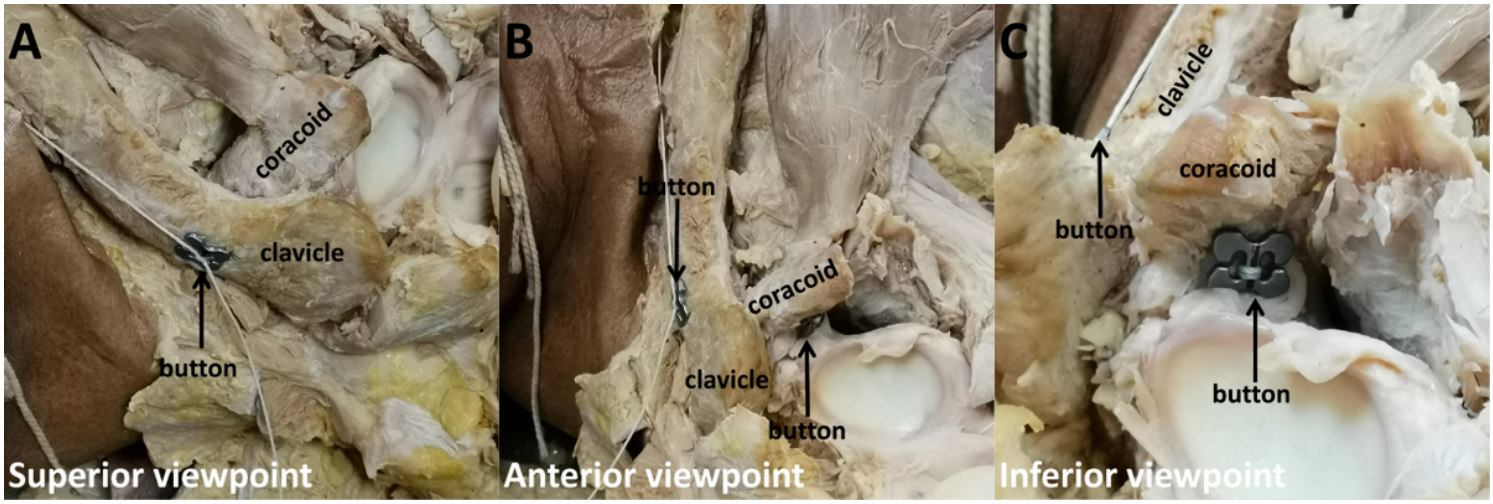


## Figure 2

Various viewpoints of the Dog Bone buttons ACJ dislocation treatment. The pictures show the surgical technique from the superior viewpoint (A), anterior viewpoint (B), and inferior viewpoint (C).

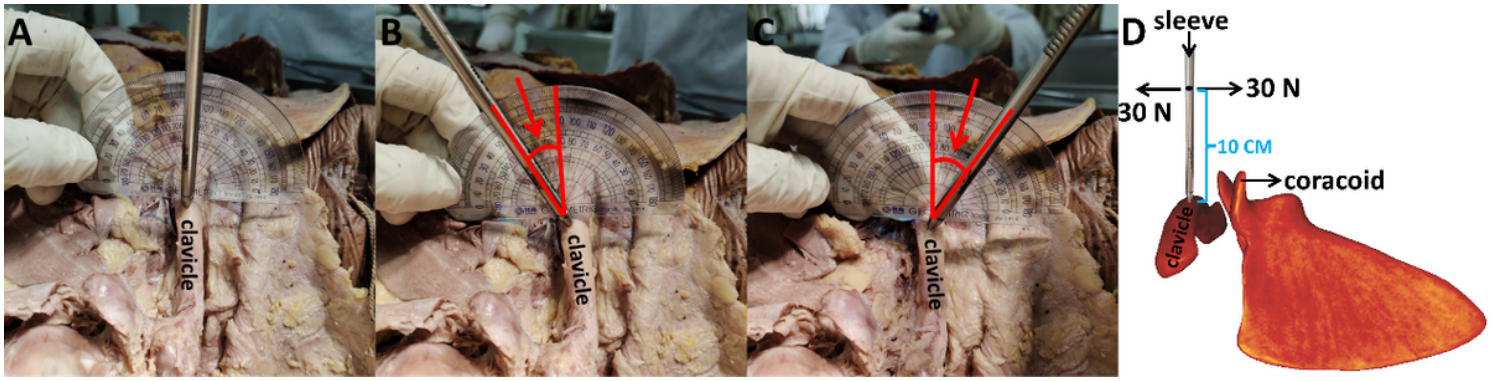


## Figure 3

The angle of pronation (A & B) and supination (A & C) of the clavicle. Pattern diagram of the cadaveric study (D).

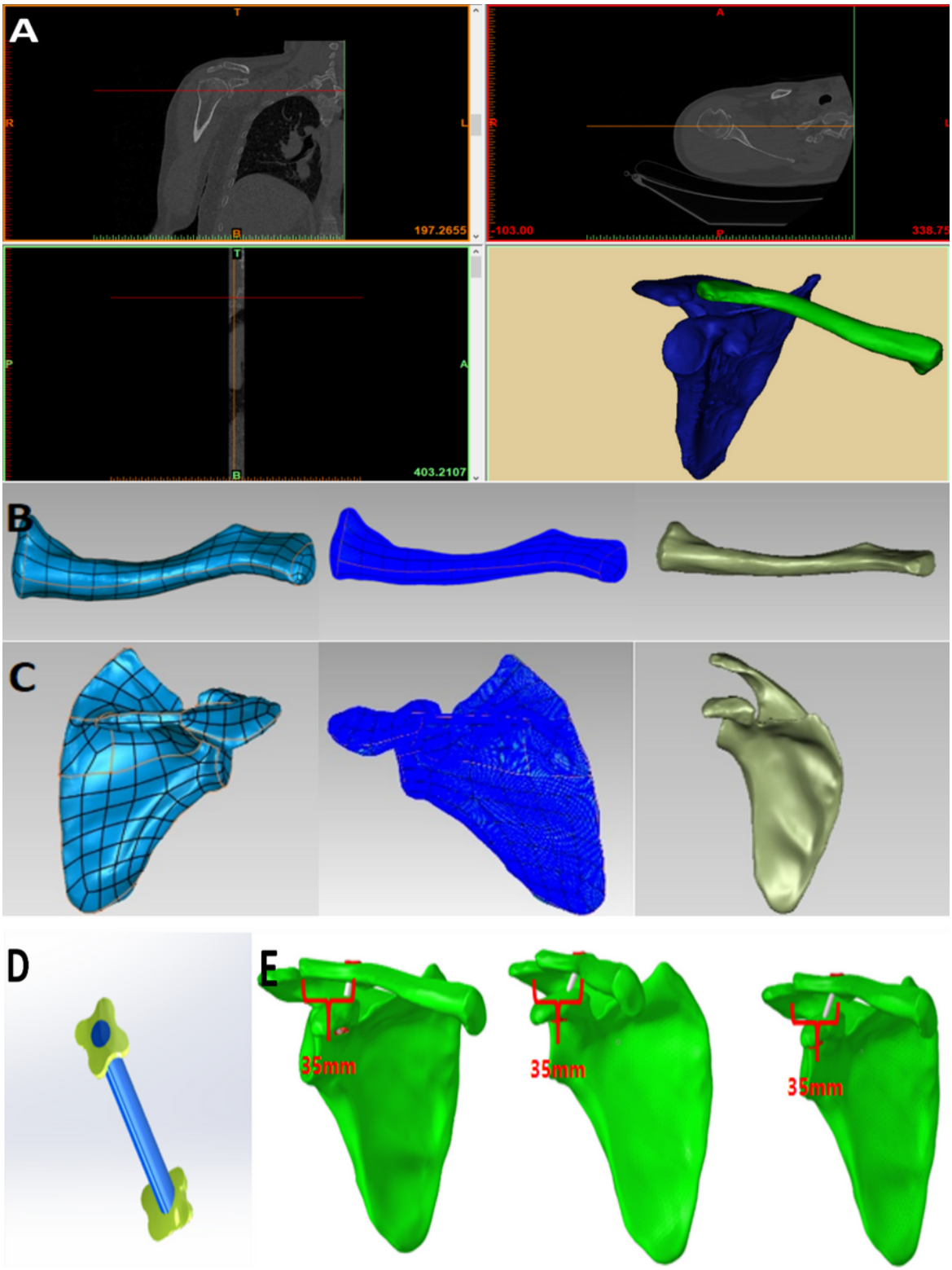


## Figure 4

Based on a CT scan of the shoulder, a DICOM image was imported into Mimics software for 3D reconstruction of the scapula and clavicle. Geomatics software was used to fit the curved surface sheet, construct grids and generate solid geometry files (A, B & C). A simplified three-dimensional model of internal fixation of the Dog Bone technique (D). Dog Bone internal fixation models have been introduced into bone models to simulate CC ligament reconstruction under the G1, G2, and G3 (E).

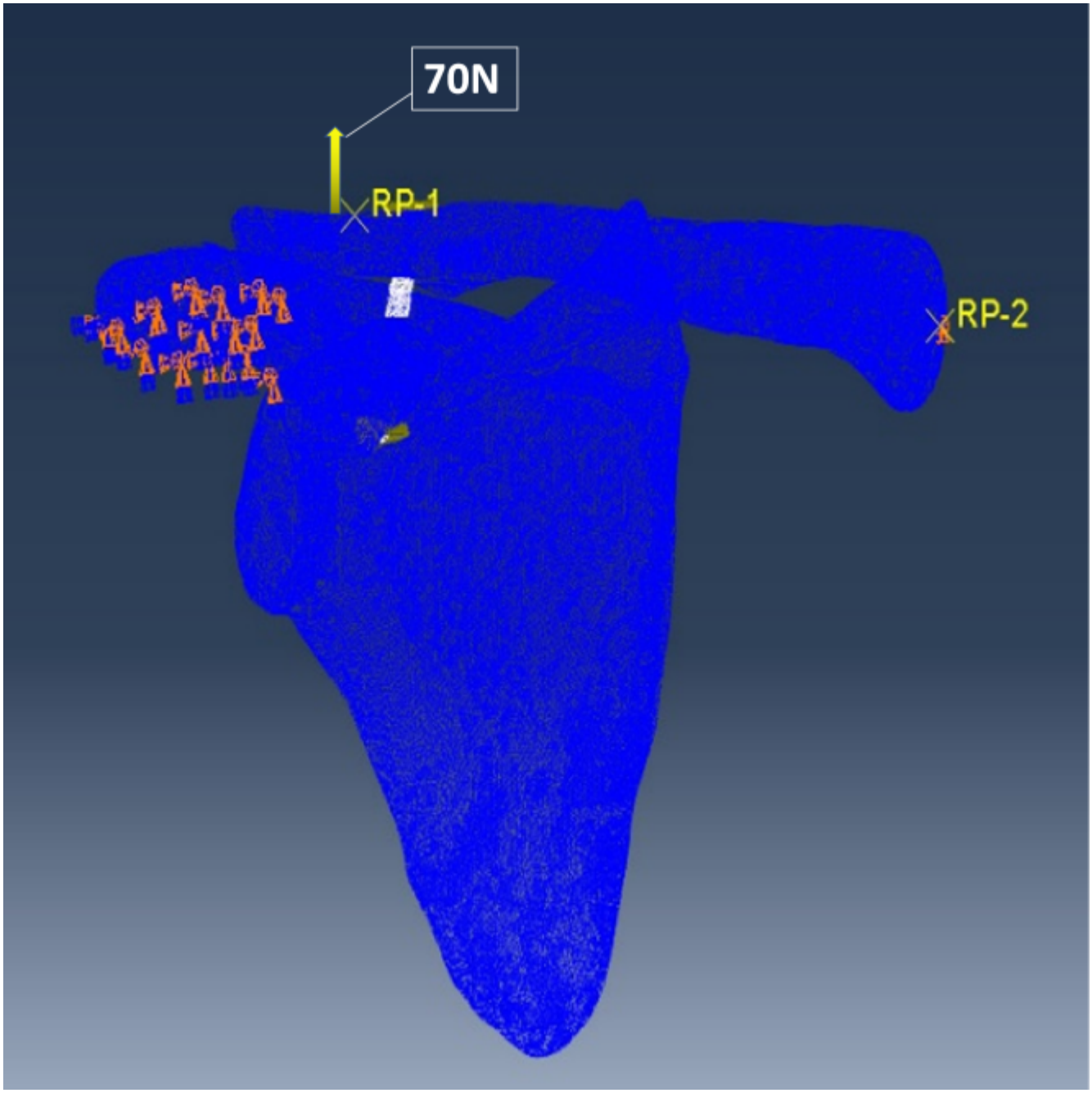


**Figure 5**

Boundary conditions were applied to the models.

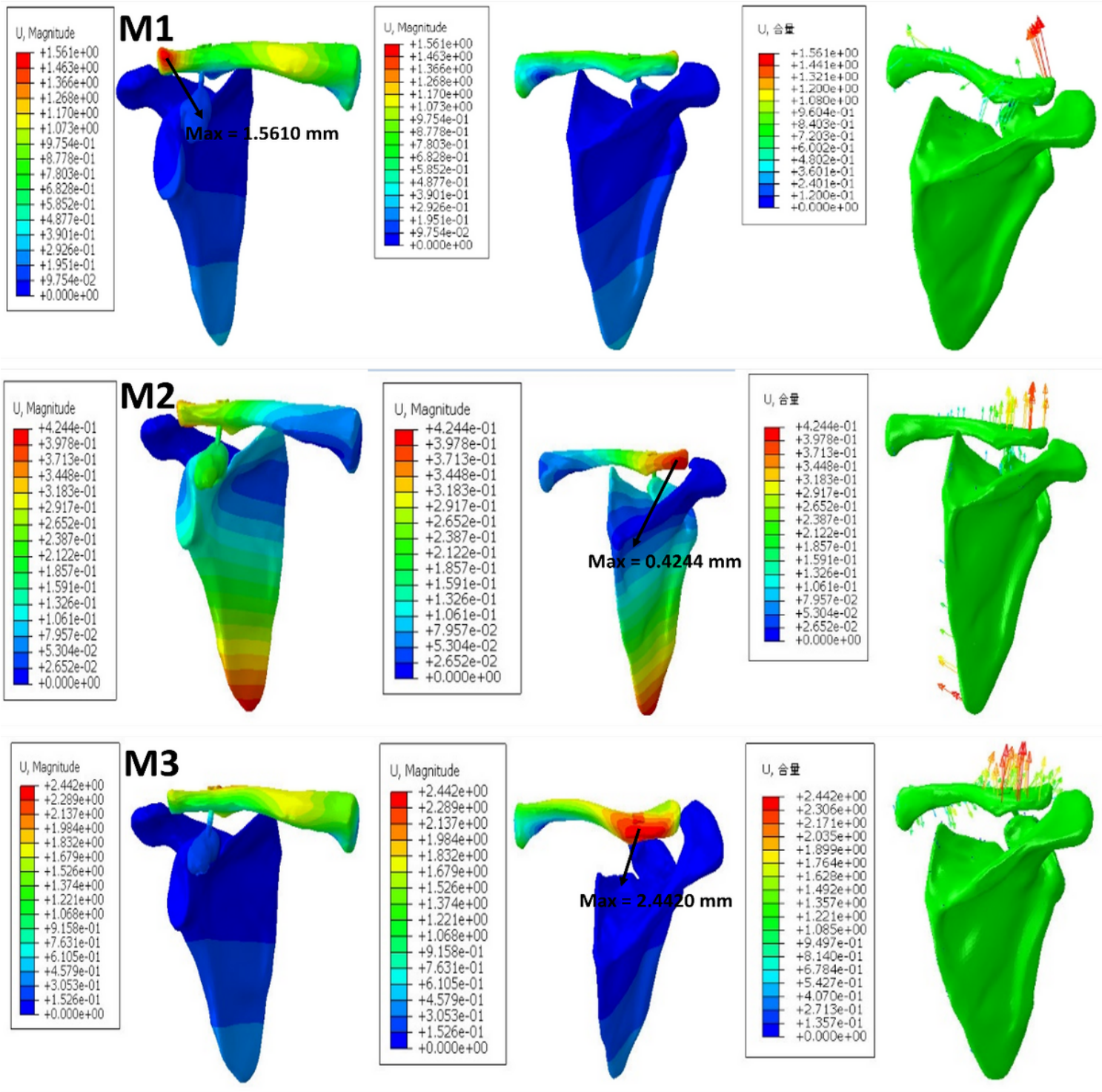


## Figure 6

Displacement nephogram of M1, M2, and M3.

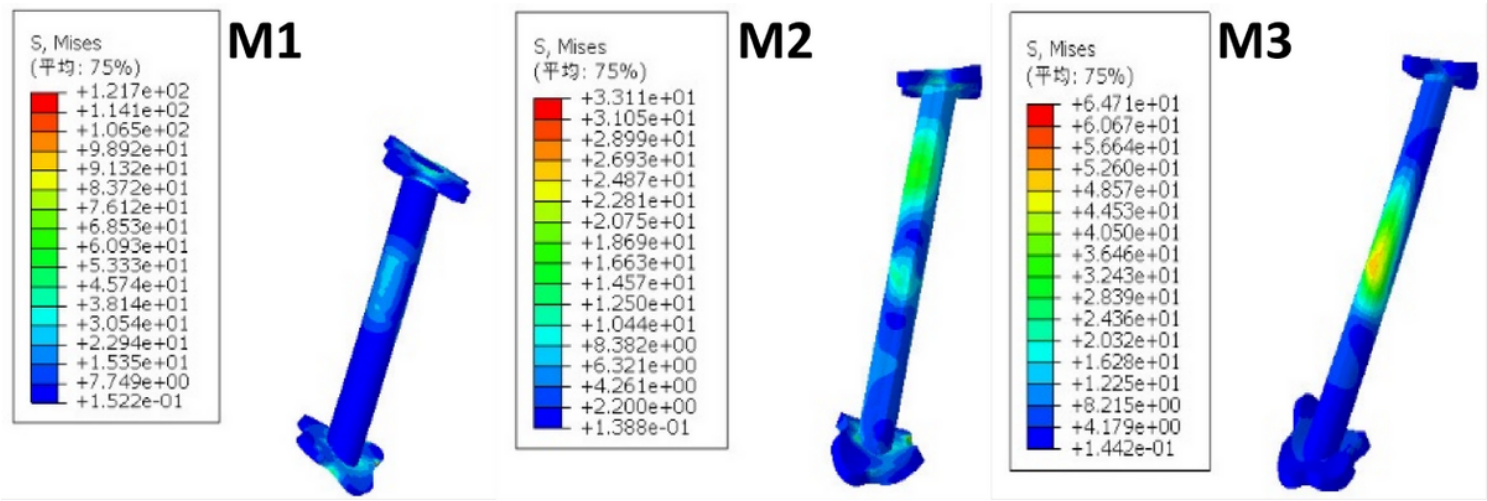


**Figure 7**

The peak value of the von Mises stress along the FiberWire in M1, M2, and M3.

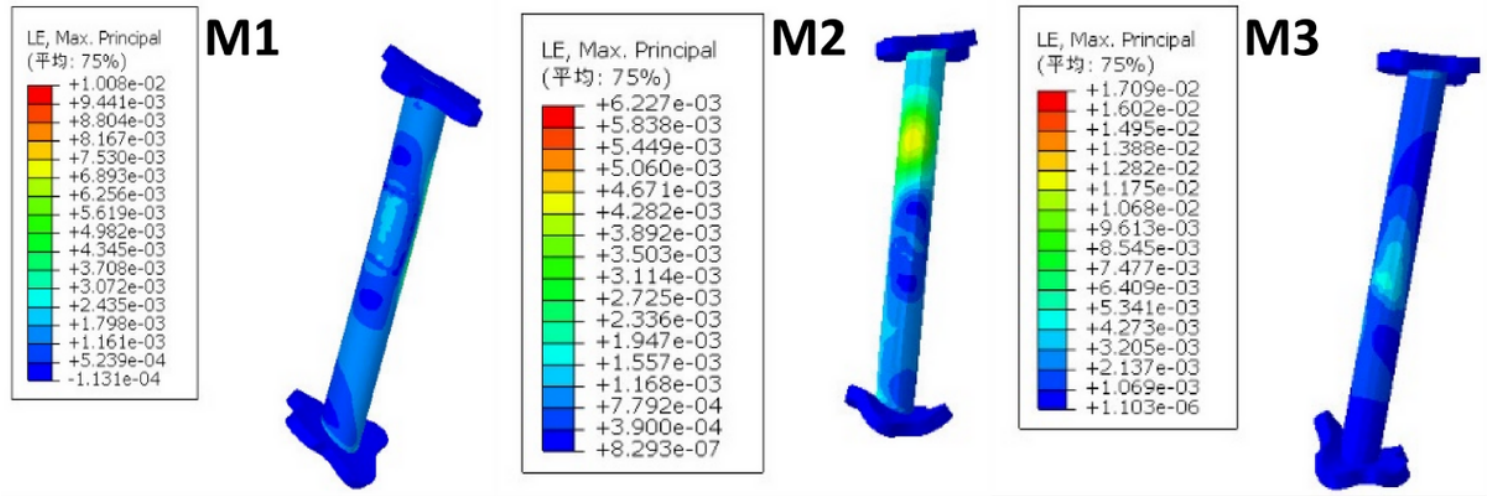


**Figure 8**

The strain LE along the FiberWire in M1, M2, and M3.